UC San Diego
UC San Diego Previously Published Works

Title

Identifying the drivers of structural complexity on Hawaiian coral reefs

Permalink

https://escholarship.org/uc/item/8kt2k2q2

Authors

McCarthy, OS

Smith, JE

Petrovic, V

et al.

Publication Date

2022-12-08

DOI

10.3354/meps14205

Supplemental Material

https://escholarship.org/uc/item/8kt2k2q2#supplemental

Copyright Information

Peer reviewed

1 **Title**: Identifying the drivers of structural complexity on Hawaiian coral reefs

2

3 **Authors**: Orion S. McCarthy[1*], Jennifer E. Smith[1], Vid Petrovic[2], Stuart A. Sandin[1*]

4

5 **Affiliations:**

6   1. Center for Marine Biodiversity and Conservation, Scripps Institution of Oceanography,

7   University of California San Diego, La Jolla, California 92037, USA

8   2. Department of Computer Science and Engineering, University of California San Diego,

9   La Jolla, California 92037, USA

10

11 ***Author e-mails for correspondence:** ssandin@ucsd.edu (SAS)

12

13 **Keywords**: Fractal dimension, linear rugosity, Structure from Motion, structural complexity,

14 coral reefs, geomorphology, Hawaii

15

16

17

18

19

20

21

22

23

24 **Abstract**

25

26   Habitat structural complexity is created by biotic and abiotic processes that operate over a

27 range of scales. This can be seen clearly on coral reefs, where corals and reef geomorphology

28 create structure from mm to km scales. Here, we quantify the relative contribution of biotic and

29 abiotic structures to habitat complexity using Structure from Motion, a technology that allows

30 accurate 3D models of environments to be reconstructed from overlapping photographs. We

31 calculate the linear fractal dimension of these models using a virtual analogue of a profile gauge.

32 By adjusting the spacing between profile gauge rods, we partition structural complexity into a

33 series of scale intervals. We identify scales that are most indicative of coral-cover (0.5-16 cm)

34 and reef geomorphology (16-256 cm). We find that reefs in the Main Hawaiian Islands have

35 more complexity at finer scales than reefs in the Northwest Hawaiian Islands, which we attribute

36 to the latitudinal gradient in coral cover along the archipelago. At coarser scales, islands at each

37 end of the archipelago have sites with high structural complexity, with less complexity in the

38 center of the archipelago. These differences are consistent with geologic factors shaping island

39 uplift, subsidence, and reef formation. In addition, we find that different coral genera and

40 morphologies display unique patterns of fractal dimension, with branching *Porites* corals

41 creating the greatest amount of habitat structure at nearly all scales. This study demonstrates how

42 multi-scale approaches can be used to identify the processes responsible for reef structural

43 complexity and changes in structure over time.

44

45

46

1. Introduction

In many ecosystems, there is a strong relationship between species diversity and the structural complexity of the associated habitat (Henderson & Robertson 1999, Tews et al. 2003, Graham 2004, Ishii et al. 2004, Graham & Nash 2013), and coral reefs are no exception. Among the most biodiverse ecosystems on the planet (Knowlton et al. 2010, Plaisance et al. 2011), coral reefs are an amalgamation of abiotic and biotic structure shaped by the growth and accretion of scleractinian corals (Grigg 1998, Perry & Álvarez-Filip 2019), hydrodynamic forces (Dollar 1982, Donovan et al. 2018, Levenstein et al. 2022), and island evolution (Clague 1996, Kench & Mann 2017). Numerous studies have demonstrated a relationship between reef structure and coral cover and morphology (Álvarez-Filip et al. 2011, Graham & Nash 2013, Darling et al. 2017). The substrate of a coral reef forms a patchwork of holes, crevices, overhangs, and other refugia of various sizes, which in turn serves as habitat for fish and invertebrates across a range of scales (Friedlander & Parrish 1998, Wilson et al. 2007, González-Rivero et al. 2017).

Structural complexity can be defined as the diversity and arrangement of habitat structure in both the vertical and horizontal direction (Tokeshi & Arakaki 2012). On coral reefs, structural complexity has been found to be a predictor of herbivory (Vergés et al. 2011, Santano et al. 2021, but see Oakley-Cogan et al. 2020), reef fish assemblage variation (Harborne et al. 2012, González-Rivero et al. 2017, Ferrari et al. 2018), and reef resilience and recovery potential (Graham et al. 2015, Burns et al. 2016). Furthermore, changes in structural complexity due to climate-driven losses in coral cover are expected to negatively impact coral reef biodiversity in the coming decades (Bozec et al. 2015). Thus, measuring structural complexity can serve as a proxy for other aspects of reef condition, including habitat quality and benthic community

70 composition, while repeated measurements can enable scientists, reef managers, and

71 conservation practitioners to track changes in reef condition over time.

72   Given the ecological importance of structural complexity on coral reefs, scientists have

73 invested considerable time and energy to develop and refine methods for quantifying the three-

74 dimensional structure of these habitats. Linear rugosity, the ratio of the contour distance across a

75 surface to the linear horizontal distance that contour traverses, has historically been the most

76 commonly used metric to quantify structural complexity (Graham & Nash 2013, Young et al.

77 2017). Efforts to measure linear rugosity *in situ* date back to the 1970s with the advent of the

78 chain-and-tape approach (Risk 1972). Linear rugosity can also be measured *in situ* using a

79 profile gauge, an instrument that consists of a series of parallel rods in a linear frame. When

80 placed on the substrate from above, the rods slide independently to rest on the shallowest object

81 beneath, approximating the contour of the substrate along a line (McCormick 1994, Vermeij et

82 al. 2007). The spacing between profile gauge rods determines the resolution of the linear rugosity

83 measurement, and thus a profile gauge provides a scale-dependent measure of linear rugosity.

84 Although widely used, methods for measuring linear rugosity *in situ* are time consuming, prone

85 to user error, potentially damaging to the habitat, and impractical for measuring large areas of the

86 benthos across multiple scales (Storlazzi et al. 2016, Bayley et al. 2019).

87   Recently, there has been growing interest in using three-dimensional modeling to

88 quantify the structural complexity of coral reefs (D'Urban Jackson et al. 2020, Lepczyk et al.

89 2021, Ferrari et al. 2021). These studies, made possible by rapid advances in computing power

90 and data storage, use Structure from Motion (SfM) to reconstruct underwater environments using

91 the overlap between photographs (Westoby et al. 2012, Burns et al. 2015). As a type of

92 photogrammetry, SfM relies on parallax, the apparent displacement of an object when viewed

93 from multiple different directions, to reconstruct 3D scenes from 2D data (Anderson et al. 2019).

94 SfM allows researchers to conduct semi-automated "virtual field work" from these digital

95 representations of nature. This technique has the potential to transform the speed and scale at

96 which scientists measure structural complexity (Couch et al. 2021), while improving our ability

97 to make repeatable measurements and track change through time (Yuval et al. 2021). Already,

98 SfM has been used to quantify coral growth rates (Ferrari et al. 2017, Kodera et al. 2020, Sandin

99 et al. 2020), changes in structural complexity following disturbance events (Burns et al. 2016,

100 Ferrari et al. 2016), spatial heterogeneity in complexity (Leon et al. 2015), the influence of coral

101 colony morphology on complexity (Burns et al. 2015, Figueira et al. 2015), and the relationship

102 between fish abundance and structural complexity (González-Rivero et al. 2017, Ferrari et al.

103 2018).

104   One of the most promising applications of SfM is the ability to measure structural

105 complexity across a range of scales. The substrate of a coral reef is comprised of structures that

106 span several orders of magnitude in size, and these structures influence the biology and ecology

107 of reef organisms (Hatcher et al. 1987, Nash et al. 2014, Levenstein et al. 2022). For instance, the

108 way in which organisms interact with the structure of the reef depends on their body size. This

109 phenomenon, termed the textural discontinuity hypothesis, was first noted by Holling to describe

110 the size distribution of birds and mammals in relation to habitat structure (Holling 1992), and has

111 since been shown to apply to coral reef fish assemblages as well (Hixon & Beets, 1993, Nash et

112 al. 2013). Thus, it is important to consider how structural complexity varies across a range of

113 scales in order to draw ecological inferences about reef fish assemblages (Luckhurst &

114 Luckhurst 1978, Nash et al. 2014, Fukunaga et al. 2020b, Urbina-Barreto et al. 2022), mobile

115 invertebrates (Vytopil & Willis 2001, Lee 2006) and reef-scale hydrodynamics, from boundary

116   layer characteristics (Levenstein et al. 2022) to wave setup (Franklin et al. 2013, Monismith et al.

117   2013).

118   Prior to the widespread use of SfM, several studies used *in situ* methods to quantify

119   structural complexity across multiple scales. Chains with links of various sizes have been used to

120   examine the scale dependence of linear rugosity (Knudby & LeDrew 2007), and wheels of

121   varying diameter have been used to quantify the length of reef contours at different scales (Nash

122   et al. 2013, Richardson et al. 2017). SfM enables researchers to efficiently measure reef structure

123   at high resolution over a large extent of habitat with minimal effort in the field. Importantly,

124   researchers can use this data to calculate structural metrics at different scales (Bryson et al. 2017,

125   Fukunaga et al. 2020a), eliminating the need to identify a single measurement scale *in situ*.

126   While linear rugosity is the most widely used metric of coral reef structural complexity

127   (Graham & Nash 2013), fractal dimension is arguably a more relevant metric because it accounts

128   for the scale dependence of reef structure (Fukunaga et al. 2020a). Fractal dimension is a

129   measure of an object's ability to fill Euclidean space and describes the complexity of a shape

130   (Mandelbrot 1983, Sugihara & May 1990, Halley et al. 2004). In the context of linear structural

131   complexity, fractal dimension represents the rate at which the apparent length of the reef contour

132   increases as the resolution of measurement becomes finer, and can be calculated using

133   measurements of linear rugosity made at different levels of resolution (Nash et al. 2013). In

134   ecological terms, fractal dimension is related to the amount space along the reef contour that is

135   available to organisms of a certain size class, and may change depending on the scale of

136   measurement and characteristics of the underlying substrate (Sugihara & May 1990, Tokeshi &

137   Arakaki 2012). For example, if the contour of a coral colony is measured at both 1 cm and 10 cm

138   resolution, the difference between the lengths of those contours can be attributed to structural

139   features of the colony that are between 1 cm and 10 cm in size (Figure 1). In this sense, fractal

140   dimension can be used to partition complexity by scale, quantify the abundance of structures

141   (and thus habitat availability) within a given size range, and contextualize the gain or loss of

142   structural complexity over time.

143   Few studies have utilized multi-scale patterns of structural complexity to gain insights

144   into coral reef ecology, geology, and natural history. While some studies have used fractal

145   dimension to study coral reef structural complexity across multiple scales (Bradbury 1984, Nash

146   et al. 2013, Young et al. 2017, Fukunaga et al. 2020a), these studies were either limited in their

147   geographic scope or calculated a single value of fractal dimension across a large range of scales.

148   Specifically, this study addresses the following questions: 1) how does the fractal dimension of

149   the reef substrate change across scales, 2) do biotic and abiotic reef structures exhibit different

150   patterns of fractal dimension across scales, and 3) do different coral genera and growth forms

151   exhibit distinct site- and patch-scale patterns of fractal dimension? Here we use the term biotic

152   structure to refer to structure created by living or recently living benthic organisms, and the term

153   abiotic structure to refer to reef geomorphology created by either geologic or biogenic processes

154   over longer timescales (i.e., spur and groove formations, boulder fields, etc.). We demonstrate

155   that our approach can be used to identify the scale(s) where reef structure is most complex,

156   which allows us to determine the relative importance of biotic and abiotic processes in creating

157   habitat. This in turn can inform decisions about what scales are most relevant for monitoring

158   changes in coral reef structural complexity over time. To our knowledge, this study represents

159   one of the first archipelago-scale efforts to partition coral reef structural complexity into different

160   scale intervals using fractal dimension and SfM.

161

162 **2. Methods**

163

164 <u>2.1 Study design</u>

165   This analysis of biotic and abiotic drivers of structural complexity is based on data from

166 coral reefs in the Main Hawaiian Islands (MHI) and Northwest Hawaiian Islands (NWHI). The

167 Hawaiian archipelago is an ideal location for this study because it spans a gradient of latitude

168 (from 18.9°N to 28.4°N) and geologic age (from 0.4 million years [Hawaiʻi] to 29.8 million

169 years [Kure Atoll]; Clague 1996), with older high latitude reefs in the northwest and younger low

170 latitude reefs in the southeast. Millions of years of weathering, erosion, and subsidence have

171 shaped the geomorphology of older islands and atolls, which can be reasonably expected to have

172 different nearshore topography than younger islands. Similarly, coral cover varies throughout the

173 archipelago as a function of latitude: coral cover and coral growth decrease as latitude increases

174 (Vroom & Braun 2010, Jouffray et al. 2015), reaching a threshold north of Kure Atoll beyond

175 which the rate of coral growth drops below the rate of reef subsidence (Grigg 1982). Baseline-

176 surveys in the archipelago have demonstrated the effect of both geology and latitude on

177 Hawaiian benthic communities and fish assemblages (Rooney et al. 2008, Friedlander et al.

178 2009, Vroom & Braun 2010, Jouffray et al. 2015). Thus, the Hawaiian archipelago represents a

179 unique opportunity to explore the effects of biology and geomorphology on coral reef structural

180 complexity.

181   We surveyed 65 forereef sites spanning six of the MHI (Hawaiʻi, Maui, Kahoʻolawe,

182 Lānaʻi, Molokaʻi, and Oʻahu) and four atolls in the NWHI (French Frigate Shoals, Lisianski,

183 Pearl & Hermes Reef, and Kure; Figure 2). Sites were surveyed between July 2016 and August

184 2017 as part of five separate research expeditions. The distance between sites varied by island,

185 but the median distance between neighboring sites was 4.83 km, with the closest sites located

186 1.11 km apart. Sites had a mean depth of 11.3 m (range from 4.5 m to 17.7 m, SD of 2.7 m) and

187 were located on the leeward side of islands in the MHI to control for the effect of wave energy

188 on coral assemblages. We did not restrict sampling to leeward coastlines for the NWHI, since

189 past studies have found forereef zonation patterns in the NWHI to be complex and variable

190 between atolls (Vroom et al. 2005, Schopmeyer et al. 2011), suggesting that leeward vs.

191 windward exposure may not be the primary driver of benthic community composition in the

192 NWHI, as it is in the MHI. The number of sites per island was standardized by the amount of

193 nearshore habitat, using the length of an island's leeward 10 m isobath as a proxy (or total 10 m

194 isobath for the NWHI). The number of sites per island ranged from 11 (Hawai'i) to 4 (Kure,

195 Lisianski, and French Frigate Shoals; Figure S1).

196

197 2.2 Field procedures

198 We used SfM to construct a 3D model of each forereef site from underwater photographs.

199 The field procedures for establishing and photographing sites using a SfM workflow have been

200 previously documented (Sandin et al. 2020) and are only briefly described here. At each site, a

201 team of divers placed six calibration tiles to delineate the boundaries of a 10 x 10 m site (three

202 tiles per inshore site boundary; Figure S2). Divers recorded the depth of each tile and placed four

203 50 cm scale bars within the site's boundaries. Following site setup, one diver swam

204 approximately 1.5 m above the benthos carrying a custom-built camera rig. At the majority of

205 sites, the camera rig was equipped with two D7000 SLR Nikon cameras (18 mm and 55 mm

206 lenses) in Ikelite underwater housings. Sites from two expeditions were photographed using a

207 different camera setup (35 mm lens DSLR Nikon and a GoPro 11). To account for differences

208   between these camera setups, we excluded sites (n = 4) where low quality GoPro imagery led to

209   errors in model reconstruction (i.e., model warping, erroneous "floating" points). Cameras were

210   programmed to take a photograph every second, recording approximately 5,000 images per site.

211   The diver carrying the camera rig swam slowly in a gridded pattern to ensure maximal overlap

212   between successive images, and swam several meters beyond the edge of the 10 x 10 m site to

213   ensure full coverage and minimize edge distortion.

214

215   2.3 Model construction and data collection

216   Photographs from each site were used to generate a dense point cloud reconstruction of

217   the coral reef benthos using the commercially available software *Metashape* (Agisoft LLC., St.

218   Petersburg, Russia). While other SfM studies commonly convert these point clouds into "mesh"

219   reconstructions of the benthos, mesh outputs require interpolation which can introduce structural

220   error, especially in high relief areas. Since SfM cannot reconstruct regions of the reef where

221   overlap between photos is limited, the resulting point cloud is in actuality a 2.5D representation

222   of the reef surface, with empty space in areas with limited photo coverage (e.g., overhangs, the

223   interstitial space of a branching coral colony). To best account for this error and avoid

224   interpolation, we opt to measure linear rugosity directly from the point cloud itself, since the

225   point cloud represents the most geometrically accurate reconstruction of the substrate. We use

226   linear rugosity, a one-dimensional measurement of structural complexity, because linear rugosity

227   calculations require no interpolation, are easily interpretable and computationally transparent,

228   and are comparable with *in situ* approaches such as a profile gauge. Furthermore, these factors

229   make it transparent to interpret cross-scale patterns of rugosity, which is the crux of this study.

230   We analyzed the point cloud directly using a custom-built software, *Viscore* (Petrovic et

231   al. 2014). Once the point cloud for each site was constructed, we used *Viscore* to perform all

232   further postprocessing and analysis. As a precursor to any analysis, we oriented each point cloud

233   with respect to the sea surface using *in situ* depth measurements and adjusted the scale using the

234   50 cm scale bars as a reference. After scaling and orienting the point cloud, we used the Virtual

235   Point Intercept tool (VPI) to analyze benthic community composition and the Virtual Profile

236   Gauge tool (VPG) to measure structural complexity. Both VPI and VPG are designed as virtual

237   analogues of traditional *in situ* survey methods (random point intercept method and a profile

238   gauge, respectively). The mechanics of these *Viscore* tools are described in detail elsewhere (Fox

239   et al. 2019 for VPI, supplemental materials for VPG) and are described in limited detail here.

240   We used VPI to assess benthic composition within each 10 x 10 m site following a

241   stratified random sampling design. We chose these dimensions to match the footprint of our

242   rugosity measurements and because this scale has been shown to be sufficient to capture benthic

243   patchiness and taxonomic heterogeneity on coral reefs (Palma et al. 2017). For this study, we

244   divided each site into a 32 x 32 cell grid and used VPI to identify a single random point from

245   within each grid cell, resulting in approximately 10 points/m^2 (Dumas et al. 2009, Figure S3). A

246   single researcher with training in Hawaiian benthic taxonomy identified the substrate under each

247   random point by referencing the raw imagery used to generate the point cloud. We identified

248   points to the finest taxonomic resolution possible, typically either to genus or species level, and

249   then grouped these IDs into one of six functional categories: turf algae, macroalgae, crustose

250   coralline algae, sand, coral, or other. The "other" category included cryptic encrusting organisms

251   not considered to contribute meaningfully to structural complexity on Hawaiian reefs (primarily

252   zoanthids, sponges, and tunicates), and only once exceeded 1% of the total benthic cover. For

253   points landing on coral, we recorded the growth form of the colony as well (branching,

254   encrusting, massive, plating, or corymbose).

255   We used VPG to measure the structural complexity of each site. To mimic a profile

256   gauge (McCormick 1994), VPG drops virtual rods orthogonally from the plane describing the

257   sea surface onto the point cloud below (Figure 1). Each rod records the depth of the first (i.e.,

258   shallowest) point encountered in the point cloud at the given two-dimensional coordinate. Virtual

259   rods are arranged continuously along a transect, and the spacing between the center of each rod

260   is equivalent to the resolution of the profile gauge. The contour distance along each profile gauge

261   is simply the sum of the Euclidean distances between adjacent rod termini. We calculated the

262   linear rugosity for each profile gauge by dividing the contour distance by the length of the profile

263   gauge. To minimize the impact of substrate slope on rugosity, we measured reef contours in the

264   alongshore rather than inshore direction (Figure S7). We measured reef structure using 100

265   virtual profile gauges per site, each with a resolution of 0.5 cm. Profile gauges were 10.24 m

266   long to enable data sub setting by a base two geometric series (to simulate 10 different

267   resolutions of measurement, from 0.5 cm to 256 cm) and were spaced 10.24 cm apart. These

268   settings were chosen to assess the structural complexity of benthic communities across a range of

269   scales: 10.24 m profile gauges are long enough to intersect numerous coral colonies or other

270   structural features, and the minimum resolution of 0.5 cm is detailed enough to capture intra-

271   colony detail while approaching the resolution limits of the point cloud. Sub-setting profile

272   gauges via a base two geometric series from 0.5 cm to 256 cm created equivalent scale intervals

273   on the log-log plot of linear rugosity vs. resolution, which simplified calculations of fractal

274   dimension (Nash et al. 2013). The choice of 100 transects per site reflected a tradeoff between

275   exhaustive sampling and computational efficiency. For each site, we averaged the linear rugosity

276   of all 100 profile gauges to obtain a single site-level value of linear rugosity at each level of

277   resolution. We did not quantify site-level variance of linear rugosity due to spatial

278   autocorrelation of neighboring profile gauges. Any gaps in the point cloud or missing depth

279   values were excluded from linear rugosity calculations (Figure S6).

280   We also measured the structural complexity of the most common coral morphotypes

281   (branching *Montipora* spp., encrusting *Montipora* spp., branching *Porites* spp., massive *Porites*

282   spp., and encrusting *Porites* spp.) and non-living substrate (dead coral skeletons and sand/rubble)

283   across a range of scales. Using a subset of our 65 models, we identified patches of reef with

284   uniform benthic composition and measured the rugosity of each patch using a 3 m long virtual

285   profile gauge.

286

287   2.4 Fractal dimension

288   We used linear rugosity measurements from 10 different levels of resolution to calculate

289   the fractal dimension (D) of the substrate. We calculated fractal dimension as $D = 1 - S$, where S

290   is the slope between each successive rugosity value on a log-log plot of linear rugosity vs. profile

291   gauge resolution (Figure 1; Sugihara & May 1990, Nash et al. 2013). Values of D range from 1

292   to 2; $D = 1$ for Euclidean shapes, where contour length is constant regardless of scale, and $D = 2$

293   for shapes where the apparent contour length increases toward infinity when measured at finer

294   and finer levels of resolution. While other studies have calculated a single value of D between

295   one fine and one coarse resolution (Fukunaga et al. 2020a), we calculated nine values of D, one

296   for each scale interval. This approach allowed us to partition structural complexity by scale and

297   frame reef structure in the context of its ecological function (i.e., habitat provisioning for

298   organisms of certain size classes; Nash et al. 2013). Before using this approach to assess the

299   fractal dimension of our SfM point clouds, we tested it using simulated data. We simulated reef

300   profiles with small-, intermediate-, and large-scale reef features of known size, and found that

301   values of D peaked in scale intervals that corresponded to the size of simulated reef structures

302   (Figure S4).

303

304   <u>2.5 Statistical analysis</u>

305   To identify the scales at which corals and reef geomorphology contribute to overall reef

306   structure throughout the Hawaiian archipelago, we constructed generalized additive models

307   (GAMs) to test the relationship between fractal dimension and three explanatory variables (coral

308   cover, RMS height, and latitude) at each scale interval. We used root mean square height (RMS

309   height), a metric that has been used to quantify topography in terrestrial settings (Shepard et al.

310   2001), as a proxy for reef geomorphology. To calculate RMS height, we calculated the distance

311   between each profile gauge rod terminus and the plane of best fit through the model, and then

312   calculated the standard deviation of these distances for each site. To test if RMS height was an

313   adequate proxy for reef geomorphology, we visually assessed the geomorphology of our models

314   and assigned each site a score between 0 (low relief) and 5 (high relief) following the methods of

315   Wilson et al. (2007). We found a strong correlation between these visual assessments of

316   geomorphology and RMS height (r = 0.865), which supports our use of RMS height as a proxy

317   for reef geomorphology. We also tested for relationships between RMS height, coral cover, and

318   latitude, and found no strong correlations between these explanatory variables.

319   We chose to use GAMs because fractal dimension exhibited a non-linear relationship

320   with our explanatory variables (coral cover, RMS height, and latitude) at certain scale intervals,

321   and based on the assumption that these variables were additive in terms of predicting our

322 response variable. We used a Gaussian error distribution and untransformed data. Smoothing

323 terms were selected through generalized cross validation, and diagnostic tests indicated that a

324 basis dimension of k = 9 was appropriate for model fit for coral cover and RMS height, while k =

325 5 was appropriate for latitude. One site with extreme RMS height (PHR 52) had high leverage

326 (Cooks distance >> 1), so we excluded it from this analysis.

327   To investigate the effect of coral morphotype on fractal dimension, we categorized sites

328 based on their most abundant coral genus and morphology, which resulted in the following

329 levels: branching *Montipora* reefs (n = 6), encrusting *Montipora* reefs (n = 12), branching

330 *Porites* reefs (n = 13), massive *Porites* reefs (n = 8), and encrusting *Porites* reefs (n = 2). We

331 excluded sites with less than 15% coral cover from this analysis based on natural breaks in our

332 data and the assumption that corals contribute only marginally to overall reef structure below that

333 percent cover threshold. We also excluded encrusting *Porites* sites, given the limited sample size

334 (n = 2).

335   We treated the categorical variables of coral morphotype as a fixed effect and tested for

336 differences in fractal dimension (D) between levels using analysis of variance. We performed a

337 one-way ANOVA at each scale interval using generalized least squares to explicitly account for

338 heterogeneity of variance between factor levels. Other ANOVA assumptions were met: the data

339 were normally distributed in almost all instances, and sites were separated by >1 km and could

340 thus be considered independent (i.e., sites were not close enough to overlap the same reef

341 structural features). To account for multiple comparisons, we used a reduced alpha value of $\alpha =$

342 0.01 to consider both GAM and ANOVA results significant, and performed Tukey's test of

343 multiple comparisons to identify differences between levels for each ANOVA fixed effect.

344 Analyses were conducted using the mgcv, nlme, multcomp, and rstatix packages in R version

345   4.0.5 (Hothorn et al. 2008, Wood 2011, Pinheiro et al. 2018, R Core Team 2022, Kassambara

346   2019).

347

348   **3. Results**

349

350   Site-level fractal dimension varied depending on the scale interval considered, but ranged

351   between 1.289 and 1.001 across all sites and scales. Overall, fractal dimension was highest at the

352   2-4 cm scale interval ($D_{2-4} = 1.145 \pm 0.064$ (± 1 SD)) and lowest at the 128-256 cm scale interval

353   ($D_{128-256} = 1.017 \pm 0.015$).

354

355   3.1 Coral cover and fractal dimension

356   We found a significant relationship between total coral cover and fractal dimension at all

357   scales finer than 16 cm (Figure 3). At these scales, adjusted R^2 values ranged from 0.584 (0.5-1

358   cm scale) to 0.666 (4-8 cm scale; Figure 4). At the finest scale intervals (0.5-4 cm), fractal

359   dimension increased monotonically with coral cover, while at coarser scales (4-16 cm) fractal

360   dimension was highest at reefs with intermediate coral cover, and lower at reefs with very high

361   or very low coral cover. For example, at the 8-16 cm scale interval, the fractal dimension of reefs

362   with >70% coral cover had comparable fractal dimension to reefs with 20% coral cover (Figure

363   3).

364   When considering only sites with >20% coral cover, fractal dimension did not exhibit a

365   significant relationship with coral cover at any scale. However, differences between sites became

366   apparent when the identity of specific corals was considered, rather than total percent coral

367   cover. Using 3 m long profile gauges to measure reef structure at the patch scale, we found

368   different patterns of fractal dimension between genera (*Porites* and *Montipora*) and growth

369   forms (branching, encrusting, and massive; Figure 5A). Branching corals in particular displayed

370   higher fractal dimension across scales than massive or encrusting corals. We found that skeletons

371   of dead corals also created reef structure; patch-scale measurements of coral skeletons produced

372   values of fractal dimension comparable to those of encrusting corals. Surveys of coral rubble and

373   sand patches produced the lowest values of fractal dimension of all benthic categories

374   considered.

375   Analysis of reef structure at the site-scale mirrored patch-scale results, with significant

376   differences in fractal dimension emerging for different coral morphotypes at seven of nine scale

377   intervals (Figure 5B; Table S1). Reefs where branching *Porites* was most abundant were most

378   structurally complex overall and had significantly higher fractal dimension than all other types of

379   reefs at three scale intervals (1-2 cm, 2-4 cm, and 4-8 cm). Conversely, branching *Montipora*

380   reefs had moderate fractal dimension at small scale intervals but the lowest fractal dimension of

381   all reef types at scale intervals larger than 4 cm. Reefs characterized by encrusting *Montipora*

382   had similar fractal dimension to branching *Montipora* reefs at small scales but were more similar

383   to branching *Porites* reefs at larger scale intervals. Finally, reefs characterized by massive

384   *Porites* had the lowest fractal dimension of all reef types at scales finer than 4 cm, but

385   increasingly high fractal dimension relative to other reefs at larger scale intervals. While patterns

386   of fractal dimension varied across scales, the maximum fractal dimension for all reef types was

387   observed in the 2-4 cm scale range (D_{2-4} = 1.240 ± 0.037 for branching *Porites*, D_{2-4} = 1.170 ±

388   0.017 for branching *Montipora*, D_{2-4} = 1.192 ± 0.030 for encrusting *Montipora*, and D_{2-4} = 1.146

389   ± 0.039 for massive *Porites*). Average coral cover differed between reef types as well: reefs

390   dominated by branching *Montipora* had the highest average coral cover (75.7% ± 6.3), followed

391   by encrusting *Montipora* reefs (56.6% ± 14.1), branching *Porites* reefs (38.9% ± 15.1), and

392   massive *Porites* reefs (26.1% ± 8.4).

393

394   3.2 RMS height and fractal dimension

395   We found a significant relationship between RMS height and fractal dimension at all

396   scale intervals coarser than 16 cm (Figure 3). At these scales, adjusted R^2 values peaked at the

397   64-128 cm scale interval ($R^2 = 0.708$). At the coarsest scale intervals, fractal dimension increased

398   with increasing RMS height until a reaching a threshold of 40-50 cm RMS height, above which

399   fractal dimension either leveled off or began to decrease.

400

401   3.3 Latitudinal trends

402   Coral cover and RMS height varied between sites and displayed regional patterns (Figure

403   2). Average coral cover was highest in the Maui Nui region (Molokaʻi: 65.6% ± 7.6, Lānaʻi:

404   57.6% ± 25.1, Kahoʻolawe: 48.1% ± 30.5, Maui: 40.8% ± 13.6) and lowest in the westernmost

405   atolls of the NWHI (Kure: 6.4% ± 3.8, Pearl & Hermes Atoll: 5.7% ± 5.8). Other islands had

406   intermediate levels of coral cover (Hawaiʻi: 17.9% ± 7.7, Oʻahu: 13.7 % ± 15.4, French Frigate

407   Shoals: 15.1% ± 19.2, Lisianski: 31.5% ± 17.4). Conversely, islands at both ends of the

408   archipelago had sites with the largest RMS height (Hawaiʻi: 36.67 cm ± 16.74, Kahoʻolawe:

409   34.55 cm ± 13.93, Lisianski: 31.62 cm ± 5.85, Pearl & Hermes: 46.50 cm ± 34.99, Kure: 36.27

410   cm ± 16.38) while islands in the middle of the archipelago had sites with the lowest RMS height

411   (Maui: 23.24 cm ± 6.62, Lānaʻi: 24.12 cm ± 7.54, Molokaʻi: 19.35 cm ± 6.89, Oʻahu: 15.55 cm ±

412   9.75, French Frigate Shoals: 23.02 cm ± 6.06)

413   Fractal dimension also varied throughout the island chain and was significantly related to

414   latitude at most scale intervals (0.5-64 cm). At these scales, low latitude reefs from Hawai'i and

415   the Maui Nui region generally had the highest fractal dimension, with the lowest fractal

416   dimension at reefs from O'ahu and intermediate fractal dimension in the NWHI (Figure 3).

417   Latitude was a significant predictor of fractal dimension at all scales that coral cover was

418   significant, and two of the four scale intervals where RMS height was significant (16-32 cm, 32-

419   64 cm).

420

421   **4. Discussion**

422

423   Studying the fractal dimension of reef contours across a range of scales can help to

424   contextualize the role of biotic and abiotic processes in creating structure on reefs. Notably, we

425   found a significant relationship between coral cover and fractal dimension at scales finer than 16

426   cm, which demonstrates that biotic processes primarily create reef structure at fine scales.

427   Conversely, we found a significant relationship between fractal dimension and RMS height, our

428   proxy for reef geomorphology, only at scales greater than 16 cm, suggesting that abiotic

429   processes are primarily responsible for creating reef structure at larger scales. Across all sites,

430   fractal dimension was highest at the 2-4 cm scale interval, and reefs overall had higher fractal

431   dimension at small scales than larger scales. Additionally, we found that increases in coral cover

432   do not necessarily correspond to increases in fractal dimension. For instance, at the 4-8 cm and

433   8-16 cm scale intervals, reefs with intermediate (30-60%) coral cover had the highest fractal

434   dimension.

435   Our results demonstrate that the influence of biotic and abiotic processes on reef

436   structural complexity can be detected across distinct and finite ranges of scales. In the Hawaiian

437   archipelago, the relative influence of biotic and abiotic processes on reef structure appears to

438   transition around the 16 cm scale (Figure 4). Previous studies have identified abrupt shifts in

439   cross-scale patterns of reef fractal dimension at a similar range of scales: between 16 cm and 32

440   cm in the Seychelles (Nash et al. 2013) and between 10 cm and 20 cm in the Great Barrier Reef

441   (Bradbury 1984). These similarities suggest that a transition zone between biotic structure and

442   abiotic structure may be a widespread characteristic of coral reefs at this range of scales,

443   although the precise boundaries of this transition zone will likely shift in response to coral

444   colony size structure and community composition. In the context of the textural discontinuity

445   hypothesis, this suggests that small and large bodied reef organisms may be interacting with

446   different structural features in their habitat, features that are created by distinct processes and

447   change in response to distinct environmental forcings.

448   Researchers should be cognizant of this transition zone. Measurements with a resolution

449   of centimeters will be more ecologically relevant for studies focused on biotic structure than

450   measurements with a resolution of decimeters or meters, which may not be able to detect fine-

451   scale structural changes. While other researchers have used remote sensing data with meter

452   resolution to characterize reef structure over large spatial extents in the MHI (Asner et al. 2021),

453   our results suggest that measurements with such coarse resolution will lack the sensitivity needed

454   to characterize many changes in biotic reef structure over time. High-resolution data collected

455   over spatial extents of 100s of square meters, such as the SfM models used here, provide the

456   resolution needed to track fine-scale changes in reef structure over ecologically relevant areas.

457   Integrating these data with LIDAR or satellite-based remote sensing (Swetnam et al. 2018, Deng

458   et al. 2019, Slocum et al. 2020) could enable researchers to answer additional questions across an

459   even broader range of scales (i.e., entire coastlines to islands). However, when used in isolation,

460   these coarser-scale remote sensing approaches appear to be insufficient for characterizing biotic

461   structural change on reefs.

462   It is important to note that using fractal dimension to quantify coral reef complexity does

463   not mean that coral reefs are fractal structures (Halley et al. 2004). For an object to be considered

464   fractal, it must exhibit self-similarity and scale invariance, meaning that any part of the object

465   must resemble the entire object and that patterns reoccur across scales (Mandelbrot 1983, Purkis

466   et al. 2006). By this definition, coral reefs are not fractals: reefs are composed of a diversity of

467   biotic and abiotic structures that are not self-similar (i.e., a corallite doesn't necessarily resemble

468   a coral colony). Additionally, our results demonstrate that rugosity does not exhibit a power law

469   relationship with measurement resolution across all scale intervals (Figure 5), which violates the

470   condition of scale invariance for fractals. Instead, the departure from a true power law

471   relationship that we observed in this study indicates that more structural complexity exists at

472   certain scale intervals than others. However, while objects in nature are rarely if ever truly

473   fractal, they may exhibit fractal properties across a finite range of scales (Halley et al. 2004,

474   Purkis et al. 2006).

475   We utilized a fractal approach to identify the relative contribution of coral cover and

476   geomorphology to overall reef structure across a latitudinal gradient in the Hawaiian archipelago.

477   With the exception of Oʻahu, the MHI had greater fractal dimension than the NWHI at scales

478   associated with coral cover (smaller than 16 cm). This is consistent with our benthic cover

479   analysis, which showed that Molokaʻi, Lānaʻi, Maui, and Kahoʻolawe had the highest levels of

480   coral cover in the island chain, while atolls in the NWHI had low or intermediate coral cover.

481 Despite having some of the most pristine reefs in the world, the NWHI are characterized by

482 relatively low coral cover (Friedlander et al. 2009, Vroom & Braun 2010), due in part to their

483 northerly location. Corals on high latitude reefs, such as the NWHI, face greater competition

484 with macroalgae and more extreme temperature fluctuations, factors that reduce coral growth

485 rates, accretion, and reproductive capacity (Kleypas et al. 1999, Abdo et al. 2012). However, it is

486 important to note that other studies have found coral cover in the NWHI to be patchy, with

487 concentrated areas of up to 80% coral cover in some locations and higher cover in lagoons than

488 forereef habitats (Vroom & Braun 2010). Given that our surveys were confined to the forereef of

489 four atolls, our results may not paint a complete picture of coral-driven complexity on NWHI

490 reefs.

491 The non-linear relationship between fractal dimension and latitude may be the result of

492 anthropogenic impact (i.e., low coral cover and low fractal dimension on reefs around human

493 population centers in Oʻahu) and the geologic history of the island chain. As recently as 20,000

494 years ago, the islands of Molokaʻi, Lānaʻi, Kahoʻolawe and Maui were connected as a single

495 island known as Maui Nui (Price & Elliott-Fisk 2004, Field et al. 2019). As a result of their

496 separation, the channels separating these islands are shallow and the reefs are geologically

497 young, which may explain why many of our sites from the Maui Nui region had relatively low

498 RMS height. The placement of these islands also shields their coastlines from wave energy

499 (Field et al. 2019), allowing dense monocultures of *Porites compressa* and *Montipora capitata* to

500 form in sheltered and relatively flat nearshore environments. This contrasts sharply with the

501 island of Hawaiʻi, which has steep nearshore topography and is still actively volcanizing (Clague

502 & Dalrymple 1987). This geologic history was evident in several of our sites from the south-west

503 coast, which had large boulders, steep topography, and high fractal dimension at large scales.

504   Although several sites in the NWHI also displayed steep underlying topography, the

505   geomorphology of these reefs differs from that of younger islands. The underlying volcanic rock

506   forming the NWHI has long since subsided, and is now capped by limestone from millions of

507   years of reef growth to form atolls (Rooney et al. 2008). Any extreme topography at these atolls

508   is a result of erosion or growth of the reef itself, rather than the geomorphology of the original

509   island. Baseline studies in the region have noted that islands in the northwest end of the

510   archipelago have more pronounced spur and groove geomorphology (Friedlander et al. 2009),

511   which could be a result of greater exposure to wave energy (Rooney et al. 2008). So, while reefs

512   at both ends of the archipelago have more extreme RMS height, the drivers shaping reef

513   geomorphology are likely different.

514   In addition to detecting differences in reef structure across a latitudinal gradient, we also

515   detected differences in coral-driven structure at the scale of monospecific patches and entire

516   $100m^2$ sites. Our finding that branching *Porites* creates the most structure of the selected coral

517   morphotypes is consistent with other studies (Richardson et al. 2017, Burns et al. 2019) and

518   suggests that branching *Porites* represents a keystone structure forming taxon on Hawaiian reefs.

519   Patch and site-scale results were largely consistent, with the exception of encrusting *Montipora*,

520   which had lower fractal dimension at the patch scale than the site scale. One explanation for this

521   observation is that reefs dominated by encrusting *Montipora* tended to have higher percent cover

522   of *Porites*, while reefs dominated by branching *Montipora* had almost no *Porites* cover. This

523   suggests that communities with a greater diversity of coral genera and growth forms may provide

524   greater amounts of structure than monospecific reefs, even if coral cover on monospecific reefs

525   is high. Indeed, percent cover of live corals was twice as high on branching *Montipora* reefs than

526   on branching *Porites* reefs, yet branching *Porites* reefs had higher fractal dimension at nearly all

527   scales. By examining the fractal dimension of different coral communities, we were able to

528   detect differences in structure that were not apparent when comparing reefs based on their total

529   amount of coral cover alone. Taken together, these results support the findings of past studies

530   that have found that structural complexity is not merely a function of coral cover (Álvarez-Filip

531   et al. 2011, Richardson et al. 2017, González-Barrios & Álvarez-Filip 2018, Burns et al. 2019);

532   the habitat a reef creates is dependent on the genera and growth form of its corals.

533   The ability to detect growth form and genus-specific patterns of fractal dimension is

534   important because benthic communities are dynamic and shift in response to both anthropogenic

535   and biophysical drivers (Gove et al. 2013, Jouffray et al. 2015, Jouffray et al. 2019). Donovan et

536   al. (2018) demonstrated the existence of multiple reef regimes in the MHI and found that reefs

537   may switch between regimes over time. Similarly, Rodgers et al. (2015) documented a change in

538   the relative abundance of coral species in the MHI between 1999 and 2012 (encrusting

539   *Montipora* spp. increased in abundance while *P. compressa*, the primary form of branching

540   *Porites* in Hawai'i, decreased). It is possible that community composition in the MHI has shifted

541   further since 2012, especially given that a severe bleaching event occurred in the archipelago

542   from 2014-2015 (Couch et al. 2017, Chung et al. 2019). As ocean temperatures continue to

543   warm, climate change is expected to impact benthic communities on coral reefs (Hoegh-

544   Guldberg et al. 2007, Hughes et al. 2018, Eakin et al. 2019), which may in turn impact structural

545   complexity due to a loss of total coral cover or a shift in the dominance of certain coral species

546   (Burns et al. 2016, Ferrari et al. 2016, Wilson et al. 2019). Given our findings that coral

547   skeletons contribute to overall reef structure, we expect that the scale and magnitude of structural

548   change following bleaching events (where coral tissue is lost but coral skeletons remain for

549   several years; Couch et al. 2017) would differ from disturbances such as storms (where the

550 underlying coral skeleton may be destroyed; Burns et al. 2016). Because bleaching, storms, and

551 shifts in community composition may impact reef structure and habitat availability in different

552 ways, it will be important to employ multi-scale methods to contextualize these changes over

553 time using a variety of remote sensing approaches. Furthermore, since biotic structures are likely

554 more vulnerable to climatic disturbance than abiotic structures and create structure at smaller

555 scales, our results reaffirm the need for fine-scale structural complexity measurements to assess

556 the resilience of biotic reef structure across space and time.

557

558 **5. Conclusion**

559

560   Our findings demonstrate that multi-scale analyses of structural complexity can provide

561 much needed context about the degree to which biotic and abiotic processes contribute to

562 structural complexity on coral reefs. By using fractal dimension to partition reef structure into a

563 series of scale intervals, we were able to estimate the role of corals and reef geomorphology in

564 creating reef structure across a latitudinal gradient in the Hawaiian archipelago. Interpreting

565 these findings in the context of the textural discontinuity hypothesis, our results can serve as a

566 proxy for habitat availability for reef organisms of different size classes. However, while several

567 studies have shown that the relationship between fish assemblages and reef structure is

568 dependent on body size (Friedlander & Parrish 1998, Harborne et al. 2012, Nash et al. 2013,

569 Agudo-Adriani et al. 2019), further research using fractal methods is needed to test whether the

570 textural discontinuity hypothesis holds true for reef fish assemblages across a wide range of

571 oceanographic conditions, human impacts, and geographies.

572   Furthermore, our study highlights the limitations of structural complexity studies

573   conducted at a single scale. These approaches paint a singular picture of reef structure that is

574   relevant to only one size class of reef organisms. When time or resources prevent research

575   programs from using multiple scales of measurement, care should be taken to choose the

576   appropriate scale for the ecological question at hand. However, with technological advances

577   made possible by SfM, it is increasingly practical to conduct multi-scale studies of numerous

578   ecological phenomena, including structural complexity. This study highlights how SfM can be

579   harnessed to expand the utility of existing metrics, such as linear rugosity and fractal dimension,

580   to allow us to learn something new that would not be feasible using conventional field

581   approaches. SfM will allow researchers to innovate and learn more from coral reefs than was

582   ever possible before, with direct applications to reef ecology and conservation.

583

595   valuable input during the early stages of project conception. We would also like to thank the two

596   anonymous reviewers whose feedback helped improve this study. This work was made possible

597   by the efforts of the 100 Island Challenge, which has been supported by various organizations

598   including the Scripps Family Foundation and the Moore Family Foundation. In addition, this

599   work was also supported by the Bohn Family Foundation and Orion's NSF Graduate Research

600   Program Fellowship. The authors declare no conflicts of interest.

601

602   **Literature Cited**

603

604   Abdo DA, Bellchambers LM, Evans SN. (2012) Turning up the heat: Increasing temperature and

605   coral bleaching at the high latitude coral reefs of the Houtman Abrolhos Islands. *PLoS*

606   *ONE 7*(8): e43878. 10.1371/journal.pone.0043878.

607   Agudo-Adriani E, Cappelletto J, Cavada-Blanco F, Cróquer A. (2019). Structural complexity and

608   benthic cover explain reef-scale variability of fish assemblages in Los Roques National

609   Park, Venezuela. *Frontiers in Marine Science, 6*, 1-12.

610   Álvarez-Filip L, Côté I, Gill J, Watkinson A, Dulvy N. (2011). Region-wide temporal and spatial

611   variation in Caribbean reef architecture: Is coral cover the whole story? *Global Change*

612   *Biology, 17*(7), 2470-2477.

613   Anderson K, Westoby M, James M. (2019). Low-budget topographic surveying comes of age:

614   Structure from Motion photogrammetry in geography and the geosciences. *Progress in*

615   *Physical Geography, 43*(2), 163-173.

616   Asner GP, Vaughn NR, Foo SA, Shafron E, Heckler J, Martin RE. (2021). Abiotic and human

617   drivers of reef habitat complexity throughout the Main Hawaiian Islands. *Frontiers in*

618   *Marine Science*. 10.3389/fmars.2021.631842

619   Bayley D, Mogg A, Koldewey H, Purvis A. (2019). Capturing complexity: Field-testing the use

620   of 'structure from motion' derived virtual models to replicate standard measures of reef

621   physical structure. *PeerJ, 7:e6540*. 10.7717/peerj.6540

622   Bozec Y, Álvarez-Filip L, Mumby P. (2015). The dynamics of architectural complexity on coral

623   reefs under climate change. *Global Change Biology, 21*(1), 223-235.

624   Bradbury R, Reichelt R, Green D. (1984). Fractals in ecology: methods and interpretation.

625   *Marine Ecology Progress Series, 14*, 295-296.

626   Bryson M, Ferrari R, Figueira W, Pizarro O, Madin J, Williams S, Byrne M. (2017).

627   Characterization of measurement errors using structure-from-motion and

628   photogrammetry to measure marine habitat structural complexity. *Ecology and Evolution,*

629   *7*(15), 5669-5681.

630   Burns J, Delparte D, Gates R, Takabayashi M. (2015). Integrating structure-from-motion

631   photogrammetry with geospatial software as a novel technique for quantifying 3D

632   ecological characteristics of coral reefs. *PeerJ, 3:e1077*, 1-19.

633   Burns J, Delparte D, Kapono L, Belt M, Gates R, Takabayashi M. (2016). Assessing the impact

634   of acute disturbances on the structure and composition of a coral community using

635   innovative 3D reconstruction techniques. *Methods in Oceanography, 15-16*, 49-59.

636   Burns J, Fukunaga A, Pascoe K, Runyan A, Craig B, Talbot J, Talbot J, Kosaki RK. (2019). 3D

637   habitat complexity of coral reefs in the Northwestern Hawaiian Islands is driven by coral

638   assemblage structure. *ISPRS Annals of the Photogrammetry, Remote Sensing and Spatial*

639   *Information Sciences. 42*, 61-67.

640   Chung A, Wedding L, Meadows A, Moritsch M, Donovan M, Gove J, Hunter C. (2019).

641   Prioritizing reef resilience through spatial planning following a mass coral bleaching

642   event. *Coral Reefs, 38*(4), 837-850.

643   Clague D. (1996). The growth and subsidence of the Hawaiian-Emperor volcanic chain. In D.

644   Clague, *The origin and evolution of the Pacific Island biotas, New Guinea to eastern*

645   *Polynesia: patterns and processes* (pp. 35-50). SPB Academic Publishing.

646   Clague D, Dalrymple G. (1987). *The Hawaiian-Emperor volcanic chain.* US. Geological Survey

647   Professional Paper 1350.

648   Couch C, Burns J, Liu G, Steward K, Gutlay T, Kenyon J, Eakin CM, Kosaki RK. (2017). Mass

649   coral bleaching due to unprecedented marine heatwave in Papahānaumokuākea Marine

650   National Monument (Northwestern Hawaiian Islands). *PLoS ONE, 12*(9). 10.1371/

651   journal.pone.0185121.

652   Couch CS, Oliver TA, Suka R, Lamirand M, Asbury M, Amir C, Vargas-Ángel B, Winston M,

653   Huntington B, Lichowski F, Halperin A, Gray A, Garriques J, Samson J. (2021)

654   Comparing coral colony surveys from in-water observations and Structure-from-Motion

655   imagery shows low methodological bias. *Frontiers in Marine Science, 8:647943*.

656   10.3389/fmars.2021.647943.

657   Darling E, Graham N, Januchowski-Hartley F, Nash K, Pratchett M, Wilson S. (2017).

658   Relationships between structural complexity, coral traits, and reef fish assemblages.

659   *Coral Reefs, 36*(2), 561-575.

660   Deng F, Rodgers M, Xie S, Dixon TH, Charbonnier S, Gallant EA, Vélez CML, Ordoñez M,

661   Malservisi R, Voss NK, Richardson JA. (2019). High-resolution DEM generation from

662   spaceborne and terrestrial remote sensing data for improved volcano hazard assessment -

663   A case study at Nevado del Ruiz, Colombia. *Remote Sensing of the Environment,*

664   *233(111348)*, 1-19.

665   Dollar SJ. (1982) Wave stress and coral community structure in Hawaii. *Coral Reefs, 1*, 71-81.

666   Donovan M, Friedlander A, Lecky J, Jouffray J, Williams G, Wedding L, Crowder LB, Erickson

667   AL, Graham NAJ, Gove JM, Kappel CV, Karr K, Kittinger JN, Norström AV, Nyrström

668   M, Oleson KLL, Stamoulis KA, White C, Williams ID, Selkoe KA. (2018). Combining

669   fish and benthic communities into multiple regimes reveals complex reef dynamics.

670   *Scientific Reports, 8*(1). 10.1038/s41598-018-35057-4

671   Dumas P, Bertaud A, Peignon C, Léopold M, Pelletier D. (2009) A "quick and clean"

672   photographic method for the description of coral reef habitats. *Journal of Experimental*

673   *Marine Biology and Ecology, 368(2)*, 161-168.

674   D'Urban Jackson T, Williams GJ, Walker-Springett G, Davies AJ. (2020) Three-dimensional

675   digital mapping of ecosystems: a new era in spatial ecology. *Proceedings of the Royal*

676   *Society B, 287*. 10.1098/rspb.2019.2383.

677   Eakin CM, Sweatman H, Brainard R. (2019). The 2014–2017 global-scale coral bleaching event:

678   insights and impacts. *Coral Reefs, 38*(4), 539-545.

679   Ferrari R, Bryson M, Bridge T, Hustache J, Williams S, Byrne M, Figueira W. (2016).

680   Quantifying the response of structural complexity and community composition to

681   environmental change in marine communities. *Global Change Biology, 22*(5), 1965-

682   1975.

683 Ferrari R, Figueira W, Pratchett M, Boube T, Adam A, Kobelkowsky-Vidrio T, Doo SS, Atwood

684   TB, Byrne M. (2017). 3D photogrammetry quantifies growth and external erosion of

685   individual coral colonies and skeletons. *Scientific Reports, 7*(1), 1-9.

686 Ferrari R, Malcolm H, Byrne M, Friedman A, Williams S, Schultz A, Jordan AR, Figueira W.

687   (2018). Habitat structural complexity metrics improve predictions of fish abundance and

688   distribution. *Ecography, 41*(7), 1077-1091.

689 Ferrari R, Lachs L, Pygas DR, Humanes A, Sommer B, Figueira WF, Edwards AJ, Bythell JC,

690   Guest JR. (2021). Photogrammetry as a tool to improve ecosystem restoration. *Trends in*

691   *Ecology and Evolution, 36*(12), 1093-1101.

692 Field M, Storlazzi C, Gibbs A, D'antonio N, Cochran S. (2019). *The Major Coral Reefs of Maui*

693   *Nui, Hawaii.* US Department of the Interior, US Geological Survey.

694 Figueira W, Ferrari R, Weatherby E, Porter A, Hawes S, Byrne M. (2015). Accuracy and

695   precision of habitat structural complexity metrics derived from underwater

696   photogrammetry. *Remote Sensing, 7*(12), 16883-16900.

697 Fox M, Carter A, Edwards C, Takeshita Y, Johnson M, Petrovic V, Amir CG, Sala E, Sandin

698   SA, Smith JE. (2019). Limited coral mortality following acute thermal stress and

699   widespread bleaching on Palmyra Atoll, central Pacific. *Coral Reefs, 38*(4), 701-712.

700 Franklin GL, Mariño-Tapia I, Torres-Freyermuth A. (2013). Effects of reef roughness on wave

701   setup and surf zone currents. *Journal of Coastal Research, 65(2)*, 2005-2010.

702 Friedlander A, Parrish J. (1998). Habitat characteristics affecting fish assemblages on a Hawaiian

703   coral reef. *Journal of Experimental Marine Biology and Ecology, 224*, 1-30.

704 Friedlander A, Keller K, Wedding L, Clarke A, Monaco M. (2009). A marine biogeographic

705   assessment of the Northwestern Hawaiian Islands. In A. Friedlander, K. Keller, L.

706   Wedding, A. Clarke, & M. Monaco, *NOAA Technical Memorandum NOS NCCOS 84.*

707   *Prepared by NCCOS's Biogeography Branch in cooperation with the Office of National*

708   *Marine Sanctuaries Papahanaumokuakea Marine National Monument. Silver Spring,*

709   *MD. 363 pp.*

710 Fukunaga A, Burns J, Pascoe K, Kosaki R. (2020). Associations between benthic cover and

711   habitat complexity metrics obtained from 3D reconstruction of coral reefs at different

712   resolutions. *Remote Sensing, 12*(6). 10.3390/rs12061011

713 Fukunaga A, Kosaki RK, Pascoe KH, Burns JHR. (2020). Fish assemblage structure in the

714   Northwestern Hawaiian Islands is associated with the architectural complexity of coral-

715   reef habitats. *Diversity, 12*(11), 430. 10.3390/d12110430.

716 González-Barrios FJ & Álvarez-Filip L. (2018). A framework for measuring coral species-

717   specific contribution to reef functioning in the Caribbean. *Ecological Indicaors 95*(1),

718   877-886.

719 González-Rivero M, Harborne A, Herrera-Reveles A, Bozec Y, Rogers A, Friedman A, Ganase

720   A, Hoegh-Guldberg O. (2017). Linking fishes to multiple metrics of coral reef structural

721   complexity using three-dimensional technology. *Scientific Reports, 7*(1), 1-15.

722 Gove J, Williams G, McManus M, Heron S, Sandin SA, Vetter O, Foley D. (2013). Quantifying

723   climatological ranges and anomalies for Pacific coral reef ecosystems. *PLoS ONE, 8*(4).

724   10.1371/journal.pone.0061974

725 Graham M. (2004). Effects of local deforestation on the diversity and structure of southern

726   California giant kelp forest food webs. *Ecosystems, 7*(4), 341-357.

727 Graham N, Nash K. (2013). The importance of structural complexity in coral reef ecosystems.

728   *Coral Reefs, 32*(2), 315-326.

729 Graham N, Jennings S, MacNeil MA, Mouillot D, Wilson SK. (2015). Predicting climate-driven

730   regime shifts versus rebound potential in coral reefs. *Nature, 518,* 94-97.

731 Grigg R. (1982). Darwin point: A threshold for atoll formation. *Coral Reefs, 1*, 29-34.

732 Grigg R. (1998). Holocene coral reef accretion in Hawaii: a function of wave exposure and sea

733   level history. *Coral Reefs, 17*, 263-272.

734 Halley J, Hartley S, Kallimanis A, Kunin W, Lennon J, Sgardelis S. (2004). Uses and abuses of

735   fractal methodology in ecology. *Ecology Letters, 7*(3), 254-271.

736 Harborne A, Mumby P, Ferrari R. (2012). The effectiveness of different meso-scale rugosity

737   metrics for predicting intra-habitat variation in coral-reef fish assemblages.

738   *Environmental Biology of Fishes, 94*(2), 431-442.

739 Hatcher B, Imberger J, Smith S. (1987). Scaling analysis of coral reef systems: an approach to

740   problems of scale. *Coral Reefs, 5*, 171-181.

741 Henderson P, Robertson B. (1999). On structural complexity and fish diversity in an Amazonian

742   floodplain. *Advances in Economic Botany*, 45-58.

743 Hixon MA, Beets JP. (1993). Predation, prey refuges, and the structure of coral-reef fish

744   assemblages. *Ecological Monographs, 63*(1), 77-101.

745 Hoegh-Guldberg O, Mumby P, Hooten A, Steneck R, Greenfield P, Gomez E, Harvell CD, Sale

746   PF, Edwards AJ, Caldeira K, Knowlton N, Eakin CM, Iglesias-Prieto R, Muthiga N,

747   Bradbury RH, Dubi A, Hatziolos ME. (2007). Coral reefs under rapid climate change and

748   ocean acidification. *Science, 318*(5857), 1737-1742.

749 Holling C. (1992). Cross-scale morphology, geometry, and dynamics of ecosystems. *Ecological*

750   *Monographs, 62*(4), 447-502.

751 Hothorn T, Bretz F, Westfall P. (2008). multcomp: Simultaneous inference in general parametric

752   models. *Biometrical Journal, 50*(3), 346-363.

753 Hughes T, Kerry J, Baird A, Connolly S, Dietzel A, Eakin CM, Heron SF, Hoey AS,

754   Hoogenboom MO, Liu G, McWilliam MJ, Pears RJ, Pratchett MS, Skirving WJ, Stella

755   JS, Torda G. (2018). Global warming transforms coral reef assemblages. *Nature,*

756   *556*(7702), 492-496.

757 Ishii H, Tanabe SI, Hiura T. (2004). Exploring the relationships among canopy structure, stand

758   productivity, and biodiversity of temperate forest ecosystems. *Forest Science, 50*(3), 342-

759   355.

760 Jouffray J, Nyström M, Norström A, Williams ID, Wedding L, Kittinger J, Williams G. (2015).

761   Identifying multiple coral reef regimes and their drivers across the hawaiian archipelago.

762   *Philosophical Transactions of the Royal Society B: Biological Sciences, 370*(1659), 1-8.

763 Jouffray J, Wedding L, Norström A, Donovan M, Williams G, Crowder LB, Erickson AL,

764   Friedlander AM, Graham NAJ, Gove JM, Kappel CV, Kittinger JN, Lecky J, Oleson

765   KLL, Selkoe KA, White C, Williams ID, Nyström M. (2019). Parsing human and

766   biophysical drivers of coral reef regimes. *Proceedings of the Royal Society B: Biological*

767   *Sciences, 286*(1896). 10.1098/rspb.2018.2544

768 Kassambara A. (2019). rstatix: Pipe-friendly framework for basic statistical tests. R package

769   version 0.3.1.

770 Kench PS, Mann T. (2017) Reef island evolution and dynamics: Insights from the Indian and

771   Pacific Oceans and perspectives for the Spermonde Archipelago. *Frontiers in Marine*

772   *Science, 4(145)*. 10.3389/fmars.2017.00145.

773 Kleypas JA, McManus JW, Menez LAB (1999) Environmental limits to coral reef development:

774   where do we draw the line? *American Zoologist, 39*, 146-159.

775 Knowlton N, Brainard R, Fisher R, Moews M, Plaisance L, Caley M. (2010). Coral Reef

776   Biodiversity. In N. Knowlton, R. Brainard, R. Fisher, M. Moews, L. Plaisance, M. Caley,

777   & Alasdair D. McIntyre (Ed.), *Life in the World's Oceans* (pp. 65-77). Blackwell

778   Publishing Ltd.

779 Knudby A, LeDrew E. (2007). Measuring structural complexity on coral reefs. *Proceedings of*

780   *the American Academy of Underwater Sciences 26th Symposium* (pp. 181-188). Dauphin

781   Island, A.L.: AAUS.

782 Kodera SM, Edwards CB, Petrovic V, Eynaud Y, Sandin SA. (2020) Quantifying life history

783   demographics of the scleractinian coral genus *Pocillopora* at Palmyra Atoll. *Coral Reefs,*

784   *39*, 1091-1105. 10.1007/s00338-020-01940-8.

785 Lee, SC. (2006) Habitat complexity and consumer-mediated positive feedbacks on a Caribbean

786   coral reef. *Oikos 112(2)*, 442-447.

787 Leon J, Roelfsema C, Saunders M, Phinn S. (2015). Measuring coral reef terrain roughness using

788   'Structure-from-Motion' close-range photogrammetry. *Geomorphology, 242*, 21-28.

789 Lepczyk CA, Wedding LM, Asner GP, Pittman SJ, Goulden T, Linderman MA, Gang J, Wright

790   R. (2021). Advancing landscape and seascape ecology from a 2D to a 3D science.

791   *BioScience, 71*, 596-608.

792 Levenstein MA, Gysbers DJ, Marhaver KL, Kattom S, Tichy L. Quinlan Z, Tholen HM, Kelly

793   LW, Vermeij MJA, Johnson AJW, Juarez G. (2022) Millimeter-scale topography

794   facilitates coral larval settlement in wave-driven oscillatory flow. *PLoS ONE 17(9).*

795   10.1371/journal.pone.0274088

796   Luckhurst BE, Luckhurst K. (1978). Analysis of the influence of substrate variables on coral reef

797   fish communities. *Marine Biology, 49*, 317-323.

798   Mandelbrot B. (1983). *The fractal geometry of nature.* San Francisco: Freeman.

799   McCormick M. (1994). Comparison of field methods for measuring surface topography and their

800   associations with a tropical reef fish assemblage. *Marine Ecology Progress Series, 112*,

801   87-96.

802   Monismith SG, Herdman LMM, Ahmerkamp S, Hench JL. (2013) Wave transformation and

803   wave-driven flow across a steep coral reef. *Journal of Physical Oceanography, 43(7)*,

804   1356-1379.

805   Nash K, Allen C, Angeler D, Barichievy C, Eason T, Garmestani A, Graham NAJ, Granholm D,

806   Knutson M, Nelson RJ, Nyström M, Stow CA, Sundstrom SM. (2014). Discontinuities,

807   cross-scale patterns, and the organization of ecosystems. *Ecology, 95*(3), 654-667.

808   Nash K, Graham N, Wilson S, Bellwood D. (2013). Cross-scale habitat structure drives fish body

809   size distributions on coral reefs. *Ecosystems, 16*(3), 478-490.

810   Oakley-Cogan A, Tebbett SB, Bellwood DR. (2020). Habitat zonation on coral reefs: Structural

811   complexity, nutritional resources and herbivorous fish distributions. *PLoS ONE 15*(6).

812   10.1371/journal.pone.0233498.

813   Palma M, Rivas Casado M, Pantaleo U, Cerrano C. (2017) High resolution orthomosaics of

814   African coral reefs: A tool for wide-scale benthic monitoring. *Remote Sensisng, 7(705)*,

815   1-26.

816   Perry CT, Álvarez-Filip L. (2019). Changing geo-ecological functions of coral reefs in the

817   Anthropocene. *Functional Ecology, 33*, 976-988.

818   Petrovic V, Vanoni D, Richter A, Levy T, Kuester F. (2014). Visualizing high definition three-

819   dimensional and two dimensional data of cultural heritage sites. *Mediterranean*

820   *Archaeology and Archaeometry, 14*(4), 93-100.

821   Pinheiro J, Bates D, DebRoy S, Sakar D, R Core Team. (2018). nlme: Linear and nonlinear

822   mixed effects models. R package version 3.1-137.

823   Price J, Elliott-Fisk D. (2004). Topographic history of the Maui Nui complex, Hawaii, and its

824   implications for biogeography. *Pacific Science, 58*(1), 27-45.

825   Purkis S, Riegl B, Dodge R. (2006). Fractal patterns of coral communities: evidence from remote

826   sensing (Arabian Gulf, Dubai, U.A.E.). *Proceedings of the 10th International Coral Reef*

827   *Symposium*, (pp. 1753-1762).

828   R Core Team. (2022). R: A language and environment for statistical computing. Vienna, Austria:

829   R. Foundation for Statistical Computing.

830   Richardson L, Graham NAJ, Hoey A. (2017). Cross-scale habitat structure driven by coral

831   species composition on tropical reefs. *Scientific Reports, 7*(1). 10.1038/s41598-017-

832   08109-4

833   Risk M. (1972). Fish diversity on a coral reef in the Virgin Islands. *Atoll Research Bulletin, 153*,

834   1-6.

835   Rodgers K, Jokiel P, Brown E, Hau S, Sparks R. (2015). Over a decade of change in spatial and

836   temporal dynamics of Hawaiian coral reef communities. *Pacific Science, 69*(1), 1-13.

837   Rooney J, Wessel P, Hoeke R, Weiss J, Baker J, Parrish F, Fletcher C, Chojnacki J, Garcia M,

838   Brainard R, Vroom P. (2008). Geology and geomorphology of coral reefs in the

839   Northwestern Hawaiian Islands. *Coral Reefs of the USA* (pp. 519-571). Springer

840   Netherlands.

841   Sandin SA, Edwards CB, Pedersen NE, Petrovic V, Pavoni G, Alcantar E, Chancellor KS, Fox

842   MD, Stallings B, Sullivan CJ, Rotjan RD, Ponchio F, Zgliczynski BJ. (2020).

843   Considering the rates of growth in two taxa of corals across Pacific Islands. *Advances in*

844   *Marine Biology, 87*, 167-191. 10.1016/bs.amb.2020.08.006.

845   Santano J, Milton IA, Navarro B, Warren RM, Barber PH, Fong P, Fong CR. (2021). Structural

846   complexity shapes the behavior and abundance of a common herbivorous fish, increasing

847   herbivory on a turf-dominated, fringing reef. *Journal of Experimental Marine Biology*

848   *and Ecology, 537*(151515). 10.1016/j.jembe.2021.151515.

849   Schopmeyer SA, Vroom P, Kenyon JC. (2011) Spatial and temporal comparisons of benthic

850   composition at Necker Island, Northwestern Hawaiian Islands. *Pacific Science, 65(4)*,

851   405-417.

852   Shepard M, Campbell B, Bulmer M, Farr T, Gaddis L, Plaut J. (2001). The roughness of natural

853   terrain: A planetary and remote sensing perspective. *Journal of Geophysical Research E:*

854   *Planets, 106*(E12), 32777-32795.

855   Slocum RK, Parrish CE, Simpson CH. (2020). Combined geometric-radiometric and neural

856   network approach to shallow bathymetric mapping with UAS imagery. *ISPRS Journal of*

857   *Photogrammetry and Remote Sensing, 169*, 351-363.

858   Storlazzi C, Dartnell P, Hatcher G, Gibbs A. (2016). End of the chain? Rugosity and fine-scale

859   bathymetry from existing underwater digital imagery using Structure-from-Motion (SfM)

860   technology. *Coral Reefs, 35*(3), 889-894.

861   Sugihara G, May R. (1990). Applications of fractals in ecology. *Trends in Ecology and*

862   *Evolution, 5*(3), 79-86.

863   Swetnam TL, Gillian JK, Sankey TT, McClaran MP, Nichols MH, Heilman P, McVay J. (2018).

864   Considerations for achieving cross-platform point cloud data fusion across different

865   dryland ecosystem structural states. *Frontiers in Plant Science.* 10.3389/fpls.2017.02144.

866   Tews J, Brose U, Grimm V, Tielbörger K, Wichmann M, Schwager M, Jeltsch F. (2004). Animal

867   species diversity driven by habitat heterogeneity/diversity: the importance of keystone

868   structures. *Journal of Biogeography, 31*, 79-92.

869   Urbina-Barreto I, Elise S, Guilhaumon F, Bruggemann JH, Pinel R, Kulbicki M, Vigliola L,

870   Mou-Tham G, Mahamadaly V, Facon M, Bureau S, Peignon C, Dutrieux E, Garnier R,

871   Penin L, Adjeroud M. (2022) Underwater photogrammetry reveals new links between

872   coral reefscape traits and fishes that ensure key functions. *Ecosphere, 13*(e3934).

873   10.1002/ecs2.3934.

874   Vergés A, Vanderklift M, Doropoulos C, Hyndes G. (2011). Spatial patterns in herbivory on a

875   coral reef are influenced by structural complexity but not by algal traits. *PLoS ONE, 6*(2),

876   1-12. 0.1371/journal.pone.0017115

877   Vermeij MJA, Sandin SA, Samhouri JF. (2007) Local habitat distribution determines the relative

878   frequency and interbreeding potential for two Caribbean coral morphospecies.

879   *Evolutionary Ecology, 21*, 27-47.

880   Vroom P, Page KN, Peyton KA, Kukea-Shultz JK. (2005) Spatial heterogeneity of benthic

881   community assemblages with an emphasis on reef algae at French Frigae Shoals,

882   Northwestern Hawaiian Islands. *Coral Reefs, 24(4)*, 574-581.

883   Vroom P, Braun C. (2010). Benthic composition of a healthy subtropical reef: Baseline species-

884   level cover, with an emphasis on algae, in the Northwestern Hawaiian Islands. *PLoS*

885   *ONE, 5*(3). 10.1371/journal.pone.0009733

886 Vytopil E, Willis BL. (2001) Epifaunal community structure in *Acropora* spp. (Scleractinia) on

887   the Great Barrier Reef: implications of coral morphology and habitat complexity. *Coral*

888   *Reefs, 20*, 281-288.

889 Westoby MJ, Brasington J, Glasser NF, Hambrey MJ, Reynolds JM. (2012). 'Structure-from-

890   Motion' photogrammetry: A low-cost, effective tool for geoscience applications.

891   *Geomorphology, 179(1)*, 300-314.

892 Wilson S, Graham NAJ, Polunin N. (2007). Appraisal of visual assessments of habitat

893   complexity and benthic composition on coral reefs. *Marine Biology, 151*(3), 1069-1076.

894 Wilson S, Robinson J, Chong-Seng K, Robinson J, Graham NAJ. (2019). Boom and bust of

895   keystone structure on coral reefs. *Coral Reefs, 38*(4), 625-635.

896 Wood SN. (2011). Fast stable restricted maximum likelihood and marginal likelihood estimation

897   of semiparametric generalized linear models. *Journal of the Royal Statistical Society (B),*

898   *73(1),* 3-36.

899 Young G, Dey S, Rogers A, Exton D. (2017). Cost and time-effective method for multiscale

900   measures of rugosity, fractal dimension, and vector dispersion from coral reef 3D models.

901   *PLoS ONE, 12*(4), 1-18.

902 Yuval M, Alonso I, Eyal G, Tchernov D, Loya Y, Murillo AC, Treibitz T. (2021). Repeatable

903 semantic reef-mapping through photogrammetry and label-augmentation. *Remote Sensing*, *13*(4),

904 659.

905

906

907

908

909   **Figure 1.** A) Linear rugosity is the ratio of the contour distance across a surface to the linear

910   horizontal distance that contour traverses. B) Linear rugosity can be measured using a profile

911   gauge, a tool that consists of a series of parallel rods in a linear frame. When placed on the

912   substrate, the rods slide independently to rest on the shallowest object beneath, approximating

913   the contour of the substrate along a line. The Virtual Profile Gauge tool was designed as an

914   analogue to a real profile gauge, and uses a series of virtual cylindrical rods to measure the

915   vertical height of the point cloud along virtual transects. Users can select the number of rods per

916   transect, the length of the transects, the number of transects, and the orientation of the transects

917   with respect to the point cloud. C-F) Linear rugosity is a function of the resolution of the

918   measurement instrument (i.e., the profile gauge). The rate of change in rugosity between two

919   levels of resolution (C to D or D to E) can be used to calculate fractal dimension. Fractal

920   dimension is not constant for objects that are not true fractals, and can change between different

921   scale intervals. Panel F is adapted from Nash et al. 2013.

922
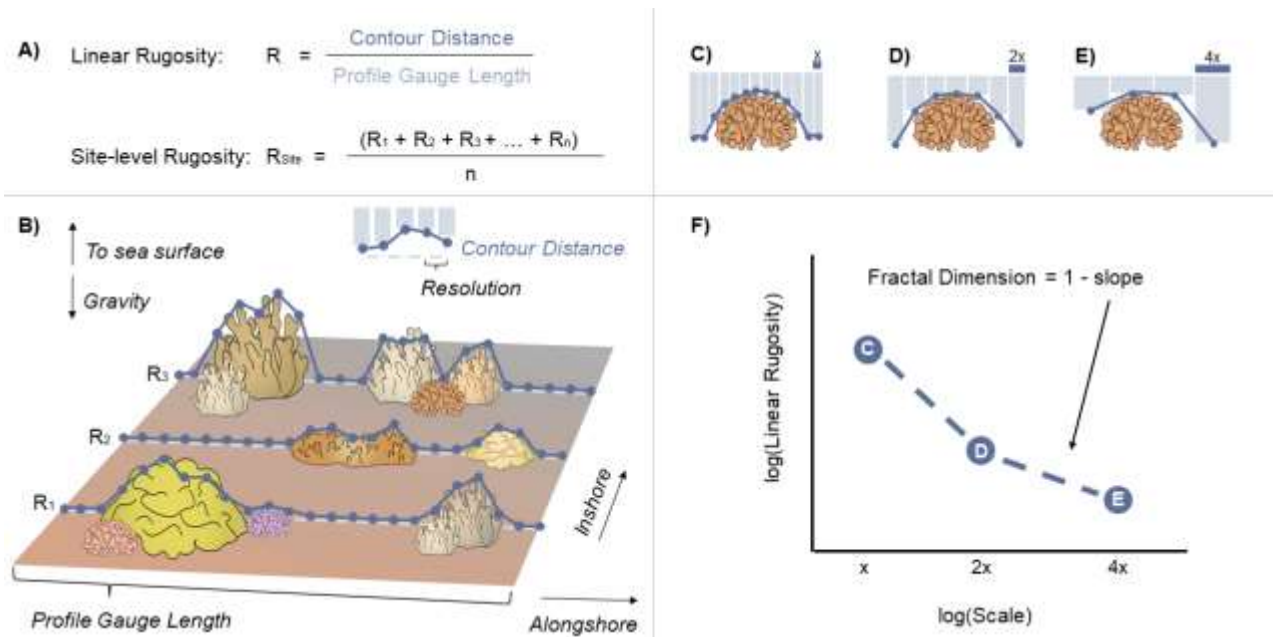
923   **Figure 2**. The Hawaiian archipelago, with labels indicating the ten islands surveyed in this study.

924   Red boxes indicate the location of inset maps, which show the location of all study sites (n = 65).

925   Sites are symbolized by coral cover (color) and root mean square (RMS) height (shape). Blue

926   lines indicate the location of the 10 m isobath around each island (leeward side only for the Main

927   Hawaiian Islands).

928

929

930
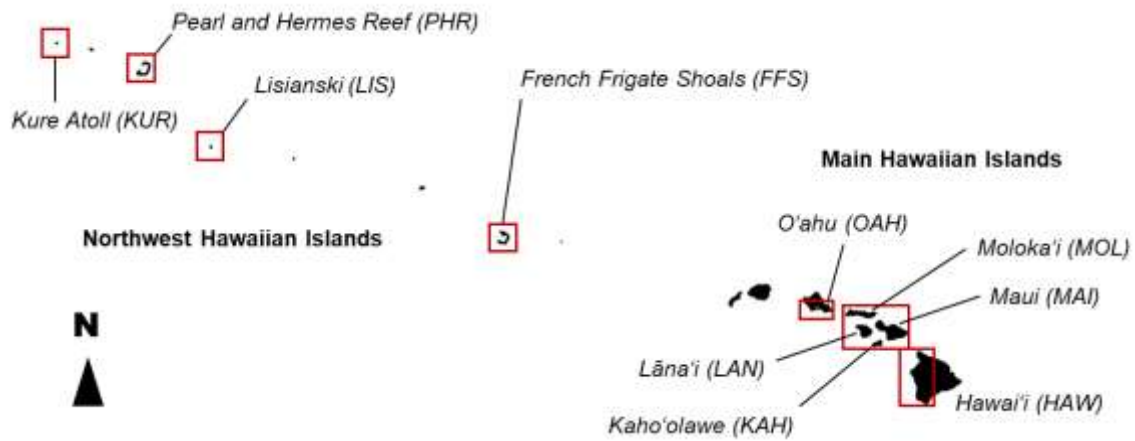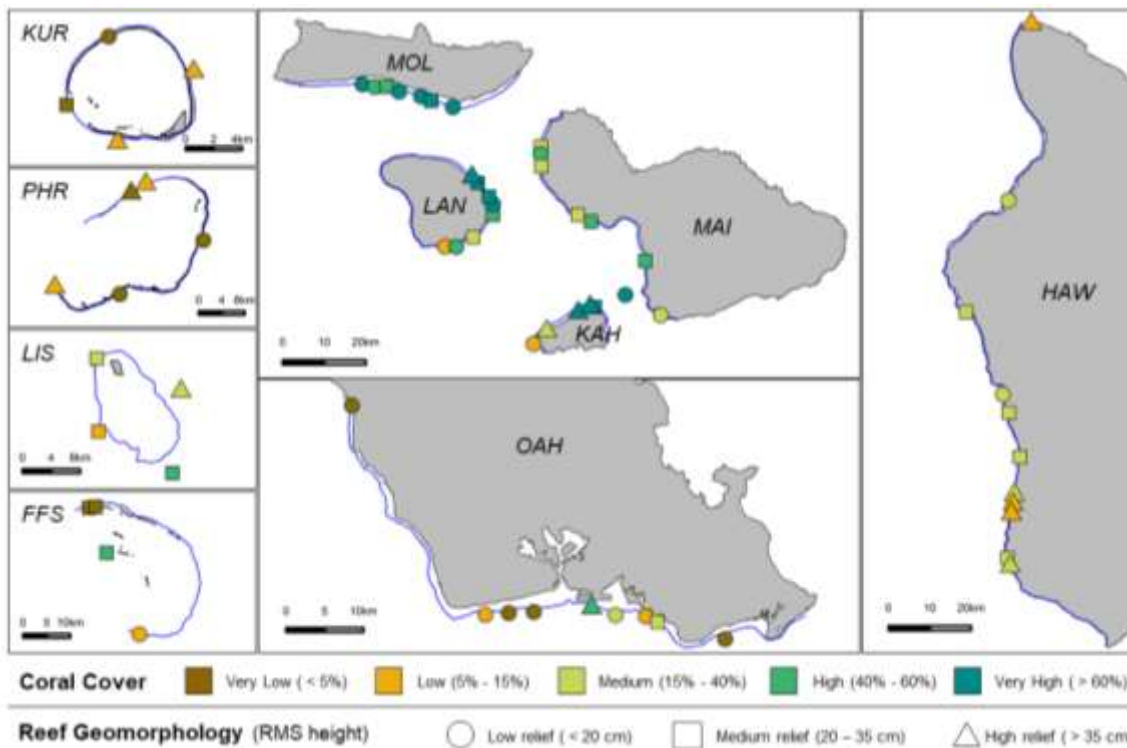
931   **Figure 3.** The partial effect of coral cover, root mean square (RMS) height, and latitude on

932   fractal dimension is shown for each scale interval. . Shading indicates significant relationships at

933   $\alpha = 0.01$ (yellow for coral cover, blue for RMS height, and red for latitude) and 95% confidence

934   intervals. Fractal dimension was significantly related to coral cover at scales finer than 16 cm,

935   and was significantly related to RMS height (a proxy for reef geomorphology) at scales coarser

936   than 16 cm. Full results are shown in Table S2.
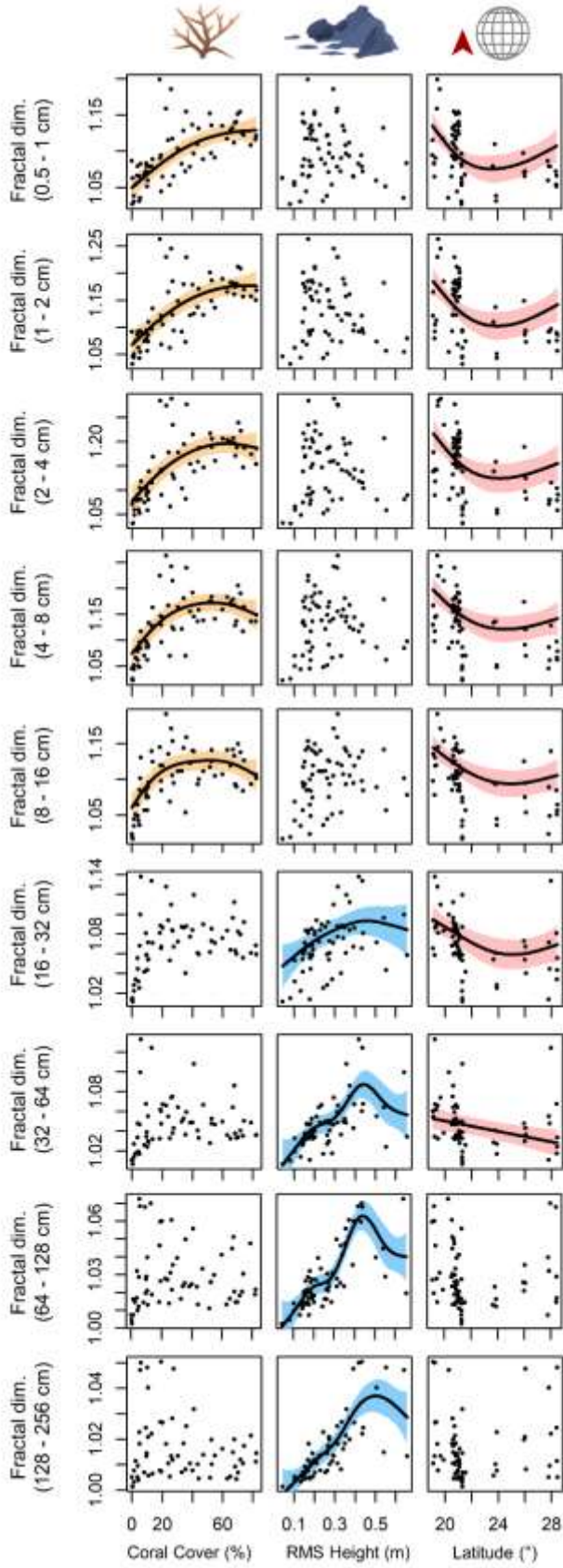
938   **Figure 4.** The adjusted R^2 value at each scale interval is shown for our GAM, which incorporates

939   coral cover, root mean square (RMS) height, and latitude as explanatory variables for fractal

940   dimension. Colors denote the scale intervals over which each explanatory variable was

941   significant (at $\alpha = 0.01$). The decline in adjusted R^2 from 16 to 64 cm indicates that neither coral

942   cover nor RMS height is a strong predictor of reef structure at intermediate scales, and that a

943   transition zone between biotic and abiotic reef structure exists in this scale range.
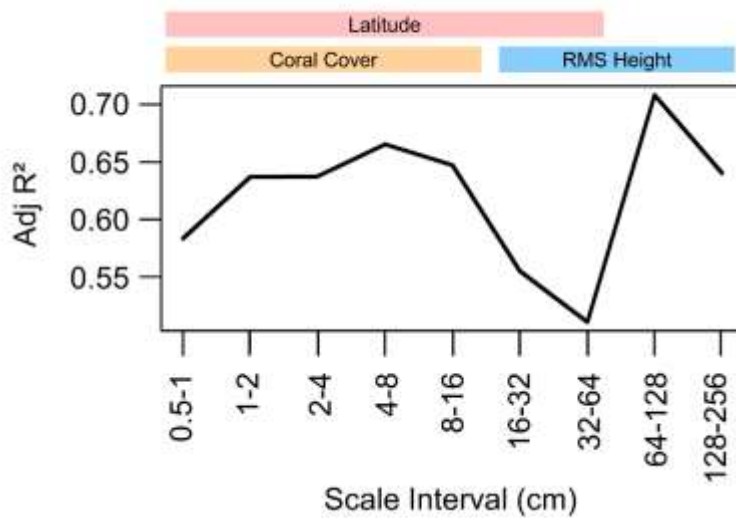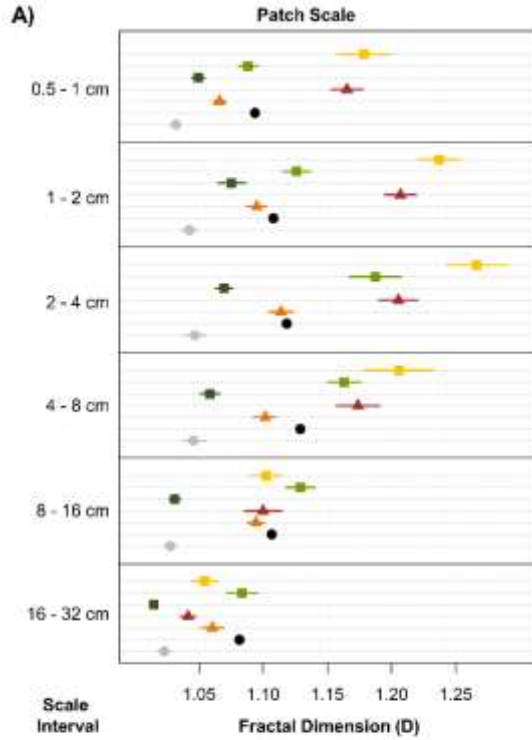

944

945

946

947

948

949

950

951

952

953

954 **Figure 5.** A) The fractal dimension of different coral morphotypes, surveyed at the patch scale

955 across six different scale intervals. B) The fractal dimension of sites based on the most abundant

956 coral morphotype at each site. Sites with >15% total coral cover were classified into one of four

957 reef types: branching *Montipora* reefs, encrusting *Montipora* reefs, branching *Porites* reefs, and

958 massive *Porites* reefs. The average percent cover for each reef type is also shown. We tested for

959 differences between reef types at each scale interval using a one-way ANOVA with generalized

960 least squares. Results were considered significant if $p < 0.01$. Differences between reef types at

961 each scale interval are signified using post-hoc letters, which were determined using Tukey's test

962 of multiple comparisons. Error bars in both panels indicate standard error.